Addressable Monolithic InSb on GaAs Focal Plane Arrays for MWIR Imaging

David R.S. Cumming
James Watt School of Engineering
University of Glasgow
Glasgow, United Kingdom
ORCID: 0000-0002-7838-8362

Vincenzo Pusino
James Watt School of Engineering
University of Glasgow
Glasgow, United Kingdom
ORCID: 0000-0002-2542-1253

***Abstract*—Mid-wave infrared sensing and imaging is of growing importance for the detection of environmental greenhouse gases such as CO_2 and CH_4. The ability to survey large infrastructure in addition to making single point measurements will bring many advantages to industrial asset management in particular. Existing technology for MWIR imaging relies on costly flip chipped technology and cryogenic cooling. We have investigated a monolithic integrated technology that can be made in a traditional planar process and operates at room temperature. By growing III-V wafers with a GaAs transistor layer and an InSb photodetection layer we are able to eliminate the need for a two-chip solution and the complex fabrication steps traditionally required. We present the method for making monolithic sensors and preliminary results demonstrating the imaging and gas sensing capabilities of the new technology.**

Keywords—Mid-wave IR, focal plane array, image sensor

I. Introduction

The CMOS focal plane array has dominated imaging and camera technology in the visible spectrum [1]. The technology provides the dual benefit of optical sensitivity, using photodiodes, and the ability to integrate all the necessary electronics to multiplex signals from large arrays of sensors. Original designs were on single chips that placed the sensor and the detection/multiplexing electronics side-by-side [2]. These chips have been superseded by two chip solutions with the electronics on one chip and the sensors on a second chip that is flip-chip bonded to the first [3]. The main benefit of this technique is that the available area for sensing is increased, thus giving greater overall sensitivity. However, the technique is not without its problems.

The general principle of making an image sensor by flip-chipping two devices together has been extended to use at wavelengths outside the visible range. Mid-wave infrared (MWIR) image sensors are made by bonding a mercury cadmium telluride (MCT) sensor device on to a silicon readout integrated circuit (ROIC). MCT is an alloy of CdTe (a semiconductor) and HgTe (a semi-metal) that forms $Hg_{1-x}Cd_xTe$ [4]. The alloy fraction x can be adjusted to give a small bandgap semiconductor that is appropriate for photoelectric detection in the MWIR. The MCT is not suitable for making electronics since devices will be leaky, and flip-chipped devices with a silicon ROIC require cooling to 77 K in order to achieve high sensitivity without saturating the detection electronics with the leakage current. Such extreme cooling puts a lot of stress on the flip-chip bonds so device lifetime is shortened [5].

We have studied an alternative technology for making a MWIR focal plane array based on indium antimonide (InSb). InSb is a III-V semiconductor with a bandgap of 0.17 eV that is suitable for photodetection in the MWIR. It can be grown using molecular beam epitaxy (MBE) and with the use of suitable lattice matching layers it can be grown directly on to large bandgap materials such as GaAs in the same growth cycle. The resulting wafer has layers that are suitable for either GaAs-based Metal Semiconductor field effect transistors (MESFETs) or InSb-based MWIR photodiodes. The two device types are monolithically integrated on to the same substrate and can withstand thermal cycling without the degradation experienced by flip-chip bonds, creating a robust and long-lived device. A further benefit is the reduction in the cost associated with a two-chip solution requiring a precision flip-chip bonding step to make the final device.

In this paper we present results on device design, formation and fabrication of arrays that are sufficiently large to support imaging applications such as thermography and gas emission detection [6]. Imaging of hydrocarbon gases and carbon dioxide are becoming increasing important for managing industrial assets and meet net-zero climate emissions targets.

II. Device Fabrication

The epitaxial layer structure used in this work is shown in Table I. The material was grown on a 3-inch semi-insulating (SI) GaAs substrate, using a molecular beam epitaxy (MBE) reactor. The growth cycle culminates in growing an InSb MWIR photodiode. The benefits of using a GaAs substrate are a cost-saving when compared to using InSb or GaSb substrates and the GaAs can be functionalised by growing the layers needed to implement MESFETs to make a multiplexor for the MWIR imaging array. The GaAs active layers consist of a silicon-doped channel layer topped by a heavily doped contact layer, both of which are n-type. To accommodate for

Table I. Epitaxial layer structure of the monolithic MWIR arrays.
0.5 µm InSb Be-doped ($7\cdot10^{17}$ cm^{-3}) p+ contact
0.02 µm AlInSb Be-doped ($7\cdot10^{17}$ cm^{-3}) p+ barrier
2.5 µm InSb non-intentionally doped absorption layer
3 µm InSb Te-doped ($7\cdot10^{17}$ cm^{-3}) n+ contact
0.3 µm undoped GaSb buffer
0.3 µm Si-doped ($2\cdot10^{18}$ cm^{-3}) GaAs MESFET n+ contact
0.2 µm Si-doped ($1\cdot10^{17}$ cm^{-3}) GaAs MESFET n- channel
0.3 µm undoped GaAs buffer
600 µm semi-insulating GaAs substrate

979-8-3503-3694-8/23/$31.00 ©2023 IEEE

the large lattice mismatch (14.6%) between GaAs and InSb, a 300-nm undoped GaSb buffer layer was grown to allow relaxation of the strain. The GaSb buffer is crucial to minimise growth defects and threading dislocations in the subsequently grown InSb photodiode (PD) layers. The InSb PD structure includes, from bottom to top, a 3-µm -thick Te-doped n+ contact layer, a 2.5-µm -thick non-intentionally doped absorption layer, a 20-nm $Al_{0.85}In_{0.15}Sb$ barrier layer, and a 500-nm-thick Be-doped p+ contact layer. The barrier layer was shown to reduce the dark current in the PD, by minimising the flow of thermally-generated electrons to the absorption region.

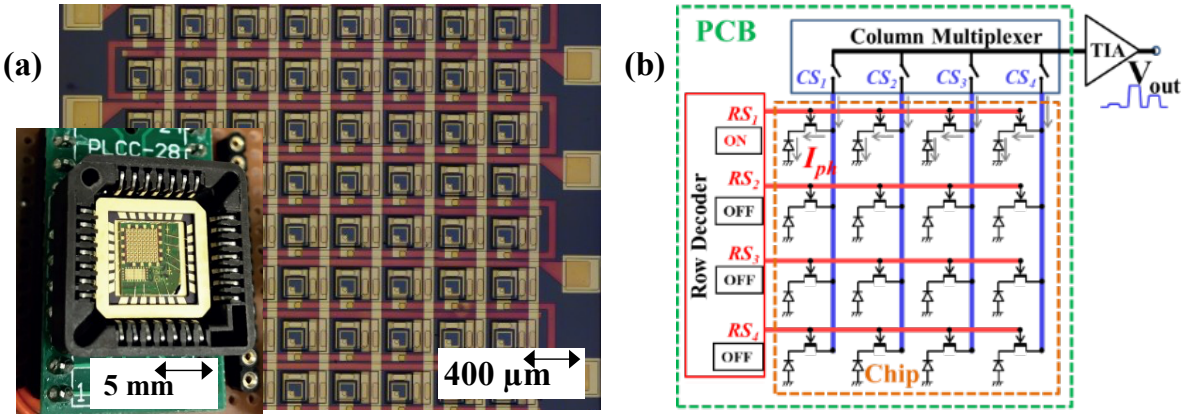

Figure 1. (a) Photograph of 8x8 monolithic array mounted in leadless chip carrier and optical micrograph of device layout. (b) Schematic of the array-addressing circuit of the monolithic array.

The fabrication of the MWIR imaging array consisted of ten post-growth fabrication steps, carried out with photolithography for increased throughput and aimed at realising identical monolithic pixel structures as the ones shown in Fig. 1(a). The processes used never exceeded 180 ºC to avoid material degradation, and wet-etching techniques were preferred to dry-etching to avoid plasma-induced damage. Mesa structures for the InSb PD and the GaAs MESFET were defined through several wet-etching steps, while metal deposition and lift-off steps were used to define the Ohmic contacts and the metal interconnections realising the rows and columns of the imaging array. The sidewalls of the InSb PD were passivated with a 600-nm-thick silicon nitride layer, shown to help reducing the leakage current in the PD [7]. To ensure the continuity of interconnections between pixels despite the non-planarity of the structure, polyimide was used as a planarisation layer [8]. Once fabricated, the array chips were mounted and bonded to ceramic leadless chip carriers for characterisation. Several formats of monolithic MWIR arrays were realised: 4x4 and 8x8 pixel arrays with a pixel size of 400 x400 µm and fill-factor of 14 % [9].

Fig. 1(b) shows a schematic of the X–Y readout scheme chosen, enabling individual addressing of the pixels and readout of the individual photocurrents. A 4x4 array is shown for simplicity, but the same read-out has been used for larger format arrays. The bonded array chip was placed on a printed circuit board (PCB), where off-the-shelf multiplexers and decoders completed the readout circuit. When biased with a sufficiently low gate-source voltage, the GaAs MESFET isolates completely the signal from the InSb PD [8]. To address each individual pixel inside the array device, the row decoder switches the corresponding MESFETs to the ON state by applying a gate-source voltage of 0 V to select a row. All GaAs MESFETs in different rows will instead be biased into the OFF state by applying a negative gate-source voltage up to -5 V. An off-chip multiplexer then reads the current of each column sequentially before the operation repeats for the next row. The photocurrent from every pixel is thus sequentially read, one-by-one. A transimpedance amplifier (TIA) converts the photocurrent output from each pixel into a voltage output.

III. Pixel Characterisation

The first step in the characterisation of the monolithic MWIR arrays was to evaluate the photocurrent spectrum of each pixel with a Fourier transform infrared (FTIR) spectrometer. Figure 2 shows the photocurrent spectra recorded from each of the 16 pixels in a 4x4 array. All pixels in the array show excellent response uniformity, important for imaging applications because sensor-to-sensor variation will result in images affected by fixed pattern noise. The photocurrent spectra show a well-defined notch near 4.26 µm wavelength, corresponding to the absorption wavelength of atmospheric carbon dioxide, since the experiments were carried out in standard atmosphere and at room temperature. The dips in the spectra near 3 and 6 µm are due to water vapour in the laboratory's atmosphere.

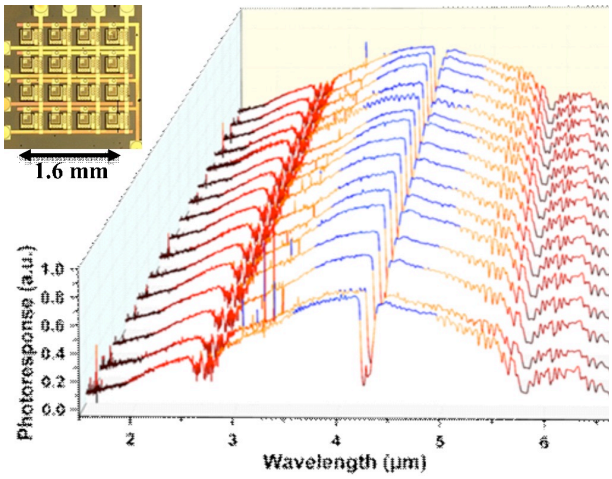

Figure 2. Photocurrent spectra from each of the 16 pixels in a 4x4 monolithic MWIR array. Inset: micrograph of the array.

The photodiodes within the pixels in the arrays could not be probed for a direct electrical characterisation of the photodiode, so stand-alone photodiodes were made and measured. The I-V characteristics at 300 K for stand-alone

photodiodes with the same layout as those in the 4x4 array (inset in Fig. 2) yielded a dark current of 13 µA at near-zero bias, increasing to 1.6 mA when applying a small negative bias (−50 mV) [9]. By making a tenfold reduction in the device size the typical leakage at 300 K can be reduced to ~1 µA at near-zero bias and 0.5 mA at −50 mV. The leakage can be reduced by up to three orders of magnitude through cryogenic cooling [7], typically employed in commercial MWIR imagers. However, modest cooling to −20 °C can

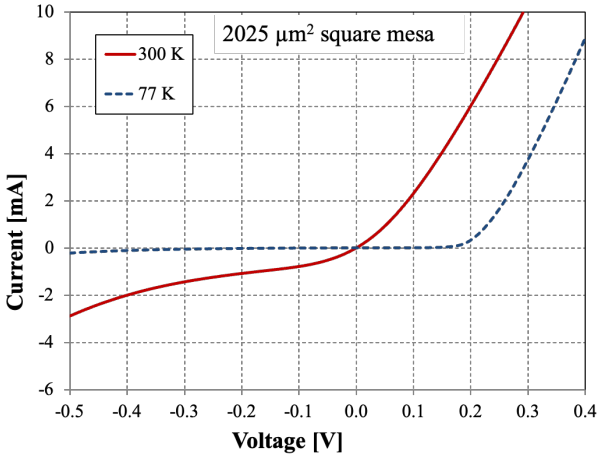

Figure 3. I-V characteristic of a p-i-n InSb photodiode at 300 K (continuous line) and 77 K (dotted line).

achieve a four-fold reduction in dark current [10], sufficient for many low-spec applications. A comparison of I-V characteristics at room temperature and at cryogenic temperature (77 K) is shown in Fig. 3 for a p-i-n InSb PD with an area of 2025 µm², corresponding to a 45x45 µm mesa size.

IV. Results and Discussion

Shadow imaging experiments were carried out to demonstrate the suitability of the arrays for MWIR imaging applications. The 4x4 array was illuminated by a Quantum Cascade Laser (QCL) emitting at 4.57 µm wavelength. The experimental set-up is described in detail in Section VI. The laser produced an elliptical beam with high divergence (30 ° vertically, 70 ° horizontally), and the 4x4 array was placed to ensure constant power across its surface plane, with the amount of available radiation comparable to atmospheric conditions [9, 11]. The incident power per pixel was ~26 µW; taking he fill factor of the pixel into account, ~4 µW of incident power were available for the pixel active area. The number of pixels (16) in the 4x4 array make it challenging to resolve an image, so a target shadowing the source QCL beam was scanned across the device to yield a composite image, shown in Fig. 4. It can be seen that the shape of the target, the tip of a tungsten electrical probe, is clearly defined.

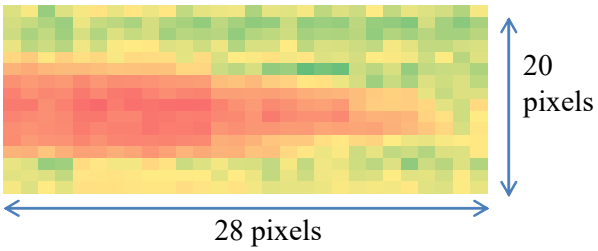

Figure 4. Image of tungsten tip obtained by combining 35 4x4 frames while scanning the tip across the 4x4 array.

To demonstrate the capability for real-time imaging as well as potential for real-world applications, the 4x4 array was used for gas-imaging experiments. As previously shown in Fig. 2, CO_2 has a well-defined absorption line in the MWIR at 4.26 µm wavelength. For gas-imaging experiments the array was illuminated by a broadband source approximating a 1200 K blackbody, filtered to let through only the absorption line of CO_2. The experiments were carried out in standard atmosphere and at room temperature, therefore a base level of ~400ppm CO_2 was already present. Fig. 5 shows the response from the 4x4 array at the beginning of the experiment (Fig. 5a), while additional CO_2 was introduced from a CO_2 cylinder (Fig. 5b), and 10 seconds later once all excess CO_2 had dispersed (Fig. 5c). The gas imaging experiment was repeated up to 80 fps, corresponding to a scanning rate of 1.28 kHz per pixel, without showing any decrease in response. The experiment was also repeated with butane gas by changing the filter of the broadband source to 3.3 µm, the main absorption line of butane, and showed similar results. The experiments proved that the monolithic 4x4 MWIR array could sense the evolution of CO_2 and butane plumes in real-time. More experiments are needed to quantify the minimum amount of gas that the pixels in the array can sense.

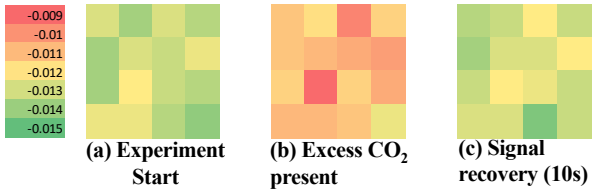

Figure 5. (a) Signal from 4x4 monolithic MWIR array at start of gas imaging experiment, (b) with excess CO_2 introduced and (c) after dispersion of excess CO_2 gas.

V. Conclusions

Monolithic InSb on GaAs FPAs were fabricated and characterised. The pixels in the array showed excellent uniformity, which makes them suitable for imaging applications. MWIR imaging was demonstrated, combining several 4x4 images to image the tip of a metal probe. Real-time imaging of gas plumes was also demonstrated with CO_2 and butane, two gases that with significance as we work towards net-zero. The results pave the way for future demonstrations of scaled-up arrays with higher imaging resolution, including 64x64 arrays with a smaller pixel size of 110 x110 µm and an increased fill-factor of 20%. Future studies on quantitative experiments of gas imaging will also be valuable.

VI. Characterisation Methods

This section describes in detail the experimental set-up for the imaging experiments with the QCL laser and for the gas imaging experiments with the broadband source.

A. Experimental set-up for shadow imaging experiments

The experimental set-up for the shadow imaging experiments with the QCL is shown in Fig. S1. The QCL used was the model 12004-2190H-C from Hamamatsu. The laser was set at a temperature of 10 °C, and driven with a constant current of 750 mA, producing a continuous wave (CW) optical power output of 60 mW at 4.57 µm wavelength. The array was placed 2.5 cm away from the QCL to ensure constant power density across its surface, thanks to its small

area (0.026 cm^2) compared to the area of the highly divergent elliptical beam from the QCL (3.7 cm^2). The 4x4 array was mounted on a PCB implementing the read-out shown in Fig. 1b. The signal output from the PCB was connected to a TIA (SR570 from Stanford Research Systems) set with a sensitivity of 10 µA/V. The output of the TIA fed into a National Instruments Digital Acquisition (NI-DAQ) system, the USB-6259, that was connected to a PC. Through a custom-made LabView code, the NI-DAQ was used both to address the pixels in the 4x4 arrays (controlling the voltages sent to

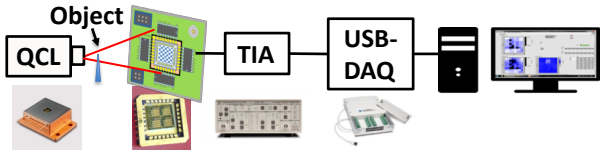

Figure S1. Experimental set-up for shadow imaging experiments.

the row decoder and multiplexer on the PCB) and to collect and display the signal from the MWIR monolithic array.

B. Experimental set-up for gas-imaging experiments

The experimental set-up for gas-imaging experiments was identical to that of Fig S1 with regards to the addressing and data acquisition set-up. There are, however, some notable difference for the optical part:

- The QCL was replaced as a source by a broadband silicon carbide (SiC) globar source approximating emission from a blackbody at a temperature of 1200 K. The source used was the model SLS203L/M from ThorLabs
- The broadband source could be fitted with an optical filter. For the experiments with CO_2, a filter with centre wavelength (CWL) of 4.26 µm, full-width at half-maximum (FWHM) of 120 nm and peak transmission of 70% minimum was used; for the experiments with butane, a filter with CWL of 3.33 µm, FWHM of 150 nm and peak transmission of 70% minimum was used.
- The gas flow was provided by a 16 g cartridge fitted with a valve for CO_2, and by a 200 ml cylinder fitted with a spray nozzle for butane.

ACKNOWLEDGMENTS

All the devices presented in this work were fabricated in the James Watt Nanofabrication Centre (JWNC). The authors would like to thank all staff within the JWNC for their assistance. This work was funded by the UK Quantum Technology Hub in Quantum Imaging, EPSRC EP/T00097X/1.

REFERENCES

[1] M. Bigas, E. Cabruja, J. Forest, J. Salvi, "Review of CMOS image sensors", *Microelectronics Journal* 37(5), 433-451, 2006. doi:10.1016/j.mejo.2005.07.002.

[2] E.R. Fossum, "CMOS image sensors: electronic camera-on-a-chip", *IEEE Transactions on Electron Devices* 44(10), 1689-1698, 1997. doi: 10.1109/16.628824.

[3] N. Watanabe, I. Tsunoda, T. Takao, K. Tanaka, T. Asano, "Fabrication of Back-Side Illuminated Complementary Metal Oxide Semiconductor Image Sensor Using Compliant Bump", *Japanese Journal of Applied Physics* 49, 04DB01, 2010. doi: 10.1143/JJAP.49.04DB01.

[4] A. Rogalski, "Mercury cadmium telluride photodiodes at the beginning of the next millennium", *Defence Science Journal* 51(1), 5-34, 2001. doi: 10.14429/dsj.51.2202.

[5] L-W. Zhang, M. Shao, X-L. Zhang, Q.-D. Meng, J-C. Wang, Y. Lv, "Three-dimensional modeling and simulation of large-format hybrid indium antimonide detector arrays", *Optical Engineering* 52(10), 103110, 2013. doi: 10.1117/1.OE.52.10.103110.

[6] M. Razeghi, B-M. Nguyen, "Advances in mid-infrared detection and imaging: a key issues review", *Reports on Progress in. Physics* 77(8), 082401, 2014. doi: 10.1088/0034-4885/77/8/082401.

[7] V. Pusino, C. Xie, A. Khalid, M.J. Steer, M. Sorel, I.G. Thayne, D.R.S. Cumming, "InSb Photodiodes for Monolithic Active Focal Plane Arrays on GaAs Substrates", *IEEE Transactions on Electron Devices* 63(8), 3135-3142, 2016. doi: 10.1109/TED.2016.2578982.

[8] C. Xie, V. Pusino, A. Khalid, M.J. Steer, M. Sorel, I.G. Thayne, D.R.S. Cumming, "Monolithic Integration of an Active InSb-Based Mid-Infrared Photopixel With a GaAs MESFET", *IEEE Transactions on Electron Devices* 62(12), 4069-4075, 2015. doi: 10.1109/TED.2015.2492823.

[9] C. Xie, M. Aziz, V. Pusino, A. Khalid, M.J. Steer, I. G. Thayne, M. Sorel, D.R.S. Cumming, "Single-chip, mid-infrared array for room temperature video rate imaging", *Optica* 4, 1498-1502, 2017. doi: 10.1364/OPTICA.4.001498.

[10] Y. Alimi, V. Pusino, M.J. Steer, D.R.S. Cumming, "InSb Avalanche Photodiodes on GaAs Substrates for Mid-Infrared Detection", *IEEE Transactions on Electron Devices* 67(1), 179-184, 2020. doi: 10.1109/TED.2019.2956283

[11] H.Yuan, X-R. Wang, B-T. Guo, K. Li, W-G. Zhang, "Modeling of the mid-wave infrared radiation characteristics of the sea surface based on measured data", *Infrared Physics & Technology* 93, 1-8, 2018. doi:10.1016/j.infrared.2018.07.005.